

Probing the ${}^8\text{He}$ ground state via the ${}^8\text{He}(p, t){}^6\text{He}$ reaction

N. Keeley^{a,*}, F. Skaza^a, V. Lapoux^a, N. Alamanos^a, F. Auger^a, D. Beaumel^b, E. Becheva^b, Y. Blumenfeld^b, F. Delaunay^b, A. Drouart^a, A. Gillibert^a, L. Giot^c, K.W. Kemper^d, L. Nalpas^a, A. Pakou^e, E.C. Pollacco^a, R. Raabe^{a,1}, P. Roussel-Chomaz^c, K. Rusek^f, J.-A. Scarpaci^b, J.-L. Sida^{a,2}, S. Stepantsov^g, R. Wolski^{g,h}

^a CEA-Saclay DSM/DAPNIA/SPhN, F-91191 Gif-sur-Yvette, France

^b Institut de Physique Nucléaire, IN2P3-CNRS, F-91406 Orsay, France

^c GANIL, Bld. Henri Becquerel, BP 5027, F-14021 Caen Cedex, France

^d Department of Physics, Florida State University, Tallahassee, FL 32306-4350, USA

^e Department of Physics, University of Ioannina, 45110 Ioannina, Greece

^f Department of Nuclear Reactions, The Andrzej Sołtan Institute for Nuclear Studies, ul. Hoża 69, PL-00681 Warsaw, Poland

^g Flerov Laboratory of Nuclear Reactions, JINR, Dubna, RU-141980, Russia

^h The Henryk Niewodniczański Institute of Nuclear Physics, PL-31342 Kraków, Poland

Received 7 July 2006; received in revised form 27 November 2006; accepted 25 January 2007

Available online 3 February 2007

Editor: V. Metag

Abstract

The weakly-bound ${}^8\text{He}$ nucleus exhibits a neutron halo or thick neutron skin and is generally considered to have an $\alpha + 4n$ structure in its ground state, with the four valence neutrons each occupying $1p_{3/2}$ states outside the α core. The ${}^8\text{He}(p, t){}^6\text{He}$ reaction is a sensitive probe of the ground state structure of ${}^8\text{He}$, and we present a consistent analysis of new and existing data for this reaction at incident energies of 15.7 and 61.3 A MeV, respectively. Our results are incompatible with the usual assumption of a pure $(1p_{3/2})^4$ structure and suggest that other configurations such as $(1p_{3/2})^2(1p_{1/2})^2$ may be present with significant probability in the ground state wave function of ${}^8\text{He}$.

© 2007 Elsevier B.V. All rights reserved.

PACS: 24.50.+g; 21.10.Jx; 24.10.Eq

Keywords: Direct reactions; Spectroscopy; CRC calculations; ${}^8\text{He}$

The ${}^8\text{He}$ nucleus has the largest neutron to proton ratio of any known particle-stable nucleus, and as such is an excellent test case for nuclear structure models at extreme values of isospin. In addition, ${}^8\text{He}$ exhibits a neutron halo or thick neutron skin [1,2]. The ${}^8\text{He}$ ground state is generally considered to have an $\alpha + 4n$ structure, the possibility of a ${}^6\text{He} + 2n$ structure being a priori ruled out on the grounds that the weak

binding energy of ${}^6\text{He}$ makes it an unsuitable core, see e.g. [3]. More concrete evidence against a ${}^6\text{He}$ core is provided by the small dipole strength obtained in a ${}^8\text{He}$ dissociation experiment [3] and the failure to satisfy the Glauber model expression: $\sigma_{-2n}({}^8\text{He}) = \sigma_I({}^8\text{He}) - \sigma_I({}^6\text{He})$ [2] where σ_I is the interaction cross section and σ_{-2n} the two-neutron removal cross section, expected to hold if ${}^6\text{He}$ and ${}^8\text{He}$ are both $2n$ halo nuclei. On the contrary, the relation: $\sigma_{-2n}({}^8\text{He}) + \sigma_{-4n}({}^8\text{He}) = \sigma_I({}^8\text{He}) - \sigma_I({}^4\text{He})$, which should hold if ${}^8\text{He}$ has a $4n$ halo structure, is rather well fulfilled by the experimental cross sections [2].

Various models of ${}^8\text{He}$ based on the $\alpha + 4n$ picture have been proposed, e.g. the microscopic multicluster model [4,5],

* Corresponding author.

E-mail address: nkeeleey@cea.fr (N. Keeley).

¹ Present address: IKS, University of Leuven, B-3001 Leuven, Belgium.

² Present address: CEA/DIF/DPTA/SPN, B.P. 12, F-91680 Bruyères-le-Châtel, France.

the cluster orbital shell model with continuum discretization [6], and the cluster orbital shell model approximation (COSMA) [7]. A ${}^8\text{He} = \alpha + {}^2n + {}^2n$ three-cluster model has also been proposed [8]. The COSMA model [7] restricts the four valence neutrons to the $1p_{3/2}$ sub-shell, quoting the more accurate calculations of [6] as justification. The microscopic multicluster model gives good agreement with the experimental ${}^6\text{He}$ transverse momentum distribution for two neutron removal from ${}^8\text{He}$ [9], as does the COSMA model [7]. The COSMA model also describes the neutron longitudinal and transverse momentum distributions in coincidence with the ${}^6\text{He}$ fragment for ${}^8\text{He}$ dissociation by Al [3], and the combined $2n$ and $4n$ removal cross sections for ${}^8\text{He} + \text{Si}$ for a range of energies [10]. The main ${}^6\text{He}$ production mechanism in high energy ${}^8\text{He}$ dissociation experiments appears to be sequential decay via the ground state of ${}^7\text{He}$, which decays exclusively into ${}^6\text{He} + n$ [3,11].

The apparent success of the COSMA model suggests that the dominant configuration in the ${}^8\text{He}$ ground state is indeed an α particle core surrounded by four valence neutrons filling the $1p_{3/2}$ sub-shell, equivalent to assuming pure jj coupling. However, the one-neutron knock out cross section for 227 MeV/u ${}^8\text{He}$ on C is overpredicted by a factor of more than 2 under this assumption [11]. The spectroscopic factor for ${}^6\text{He}$ knock-out deduced from quasi-free scattering of 671 MeV/u ${}^8\text{He}$ by a proton target is also not in agreement with the hypothesis of a closed $1p_{3/2}$ sub-shell [12].

Translationally invariant shell model (TISM) calculations suggest that the ${}^8\text{He}(p, t){}^6\text{He}$ reaction is a sensitive probe of the ${}^8\text{He}$ ground state configuration [13]. In particular, the ratio of the ${}^6\text{He } 0_1^+$ to ${}^6\text{He } 2_1^+$ contributions depends quite strongly on the assumed structure of the ${}^8\text{He}$ ground state. A DWBA analysis of ${}^8\text{He}(p, t){}^6\text{He}$ data at 61.3 A MeV [15] found a ratio of ${}^8\text{He}_{0_+} = {}^6\text{He}_{0_+} + 2n$ to ${}^8\text{He}_{2_+} = {}^6\text{He}_{2_+} + 2n$ spectroscopic factors of about unity, in agreement with the prediction of the COSMA model and the hypothesis of a closed $1p_{3/2}$ sub-shell. However, one-step [13] and two-step DWBA [14] analyses of similar data at 26 A MeV found that they could not be described using spectroscopic factors calculated using the TISM and consistent with a $(1p_{3/2})^4$ configuration for the ${}^8\text{He}$ ground state. We present an analysis of new and existing ${}^8\text{He}(p, t){}^6\text{He}$ data that yields spectroscopic factors (C^2S) in good agreement with those obtained from quasi-free scattering [12] and consistent with little or no ${}^6\text{He } 2_1^+$ contribution to the ${}^8\text{He}$ ground state.

Data for the ${}^8\text{He}(p, t){}^6\text{He}$ reaction were obtained during an experiment carried out to study the structure of ${}^8\text{He}$ by measuring the reactions induced by a 15.7 A MeV ${}^8\text{He}$ beam from the GANIL SPIRAL facility incident on a proton-rich polypropylene $(\text{CH}_2)_n$ target. The ${}^8\text{He}(p, p)$, (p, p') , (p, d) and (p, t) reactions were all measured in the same experiment by detecting the protons, deuterons and tritons in coincidence with the He fragments. Identification of the light particles and reconstruction of their trajectories and energies enabled the yields for each of the reactions: (p, p) , (p, p') , (p, d) and (p, t) to be obtained. The experimental conditions and data reduction procedure for the extraction of the (p, p) and (p, d) cross sections

are described in [16,17]. The (p, t) cross sections were obtained using the same data reduction procedure, tritons being selected in lieu of protons or deuterons. The absolute normalisation was obtained as explained in [16,17]:

- the number of incident particles was measured by two beam tracking devices providing the beam trajectory, particle by particle;
- the detection efficiency was checked through an auxiliary measurement of the $p + {}^{13}\text{C}$ elastic scattering in inverse kinematics, employing an 11.3 A MeV ${}^{13}\text{C}$ beam. It was in excellent agreement with published results obtained in direct kinematics with an 11.5 MeV proton beam incident on a ${}^{13}\text{C}$ target [18].

The normalisation of the ${}^8\text{He}(p, t)$ data has a total uncertainty of 15%. Sources of systematic error are as discussed for the ${}^8\text{He}(p, d){}^7\text{He}$ data [16,17].

The new ${}^8\text{He}(p, t){}^6\text{He}$ data, together with the existing measurement at 61.3 A MeV [15] were analysed by detailed coupled reaction channels (CRC) calculations. The aim was to obtain a good description of both data sets with the same set of spectroscopic amplitudes. All calculations were performed with the code FRESKO [19]. The following ingredients are required: scattering potentials for $p + {}^8\text{He}$, $d + {}^7\text{He}$ and $t + {}^6\text{He}$ at appropriate energies; binding potentials for $p + n$, $n + d$, ${}^2n + p$, $n + {}^7\text{He}$, $n + {}^6\text{He}$ and ${}^2n + {}^6\text{He}$; and spectroscopic amplitudes for the ${}^8\text{He}_{0_+}/{}^7\text{He}_{3/2-}$, ${}^7\text{He}_{3/2-}/{}^6\text{He}_{0_+}$, ${}^7\text{He}_{3/2-}/{}^6\text{He}_{2_+}$, ${}^8\text{He}_{0_+}/{}^6\text{He}_{0_+}$ and ${}^8\text{He}_{0_+}/{}^6\text{He}_{2_+}$ overlaps. It is the ${}^8\text{He}_{0_+}/{}^6\text{He}_{0_+}$ and ${}^8\text{He}_{0_+}/{}^6\text{He}_{2_+}$ spectroscopic amplitudes that we wish to determine from our analysis; the other ingredients may be fixed from other sources except for the $t + {}^6\text{He}$ scattering potentials, for which we make physically reasonable assumptions.

Entrance channel potentials were calculated using the JLM prescription [20], as in a previous study of the ${}^8\text{He}(p, d){}^7\text{He}$ reaction [16]. The real and imaginary normalisation factors for the JLM potentials, λ_V and λ_W , respectively, were treated as parameters, adjusted to obtain the best descriptions of the elastic scattering data by the CRC calculations. As there are no elastic scattering data available at 61.3 A MeV the result of an optical model calculation using the JLM potential with real and imaginary parts both renormalised by factors of 0.8, found to give a satisfactory description of existing ${}^8\text{He} + p$ elastic scattering data over the incident energy range 25–72 A MeV, was used as a substitute. The best fit λ_V , λ_W values obtained from the CRC calculations at 15.7 and 61.3 A MeV were 1.02, 0.22 and 0.90, 0.70, respectively.

Direct transfer of the two neutrons as a dineutron-like cluster, two-step transfer via the ${}^8\text{He}(p, d){}^7\text{He}$ reaction and coupling between the ${}^6\text{He } 0_1^+$ and 2_1^+ states were included. Excitation of the ${}^8\text{He } 2_1^+$ state was omitted as this coupling is weak. Fig. 1 gives a schematic of the coupling scheme. The ${}^8\text{He}(p, d){}^7\text{He}$ couplings were as described in Skaza et al. [16], and included deuteron breakup couplings using the CDCC formalism. The deuteron breakup space was extended to an excitation energy of 44 MeV for the calculations at 61.3 A MeV due

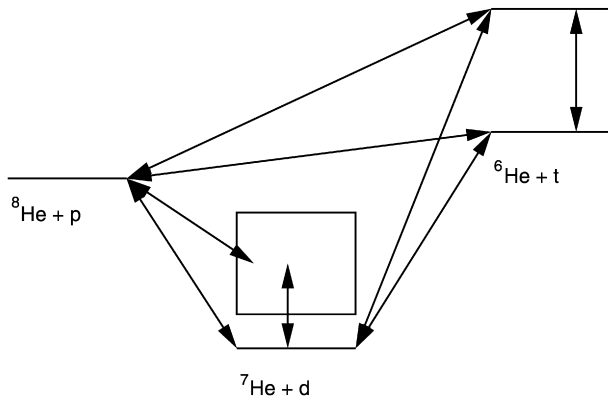


Fig. 1. Schematic of the coupling scheme used in the CRC calculations.

Table 1

$t + {}^6\text{He}$ potential parameters. The real parts are of volume Woods–Saxon form at both energies while the imaginary parts are of surface and volume Woods–Saxon form at 15.7 and 61.3 A MeV, respectively

| Energy | V | r_V | a_V | W | r_W | a_W | V_{SO} | r_{SO} | a_{SO} |
|------------|------|-------|-------|------|-------|-------|-----------------|-----------------|-----------------|
| 15.7 A MeV | 81.2 | 1.34 | 0.790 | 10.0 | 1.14 | 0.881 | 1.15 | 1.05 | 0.384 |
| 61.3 A MeV | 87.5 | 1.15 | 0.632 | 21.7 | 1.46 | 0.830 | 1.15 | 1.05 | 0.384 |

to the greater available energy (tests confirmed that additional continuum bins made a negligible difference). Unlike in Skaza et al. [16] the Koning and Delaroche global nucleon potential [21] used to construct the $d + {}^7\text{He}$ potentials at 15.7 A MeV was tuned to obtain optimum agreement with the ${}^8\text{He}(p, d){}^7\text{He}$ data at angles greater than 50° by multiplying the imaginary part by a factor of 2. As there are no ${}^8\text{He}(p, d){}^7\text{He}$ data available at 61.3 A MeV the Koning and Delaroche parameters calculated at the appropriate energy were used unchanged.

The $n + d$ and ${}^2n + p$ binding potentials were taken from [22] and [23], respectively. The $n + {}^7\text{He}$ and $n + {}^6\text{He}$ binding potentials used the “standard” parameters $R = 1.25 \times A^{1/3}$ fm, $a = 0.65$ fm; the ${}^2n + {}^6\text{He}$ binding potential employed a radius of 2.5 fm, close to the measured matter radius of ${}^8\text{He}$, and a diffuseness of 0.7 fm. All potentials were of Woods–Saxon form with depths adjusted to give the correct binding energies. The ${}^7\text{He}/{}^6\text{He}_{0+}$ form factor was calculated within a bin of width 320 keV, the potential depth being adjusted to give a resonance at the correct position above the $n + {}^6\text{He}$ threshold. Tests found that doubling the width of the bin did not affect the results.

No $t + {}^6\text{He}$ elastic scattering data are available, therefore we used ${}^3\text{He} + {}^6\text{Li}$ optical potentials in lieu. At 61.3 A MeV we used the 72 MeV type A potential of Bragin et al. [24], while at 15.7 A MeV we used potential A of Basak et al. [25]. The ${}^6\text{He} 0_1^+ \rightarrow 2_1^+$ coupling employed a collective model form factor and the isoscalar deformation length of [26], the potential parameters being adjusted to recover the no-coupling $t + {}^6\text{He}$ elastic scattering. The adjusted parameters are given in Table 1.

Spectroscopic amplitudes for the $n + p$ overlaps were as in Skaza et al. [16]. The $n + {}^7\text{He}$ spectroscopic amplitude was fixed by an analysis of the ${}^8\text{He}(p, d)$ data at 15.7 A MeV and is 12% smaller than the value given in Skaza et al. [16] due to a slight error (a parameter controlling the calculation of the non-

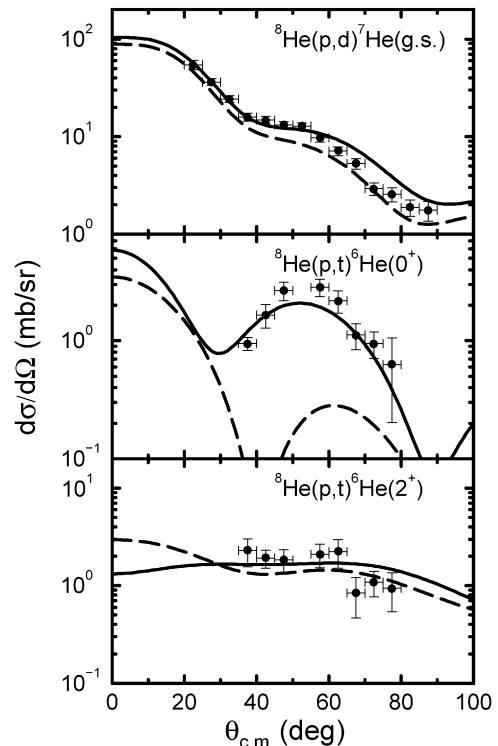


Fig. 2. CRC calculation at 15.7 A MeV compared to the ${}^8\text{He}(p, d){}^7\text{He}$ [16,17] and ${}^8\text{He}(p, t){}^6\text{He}$ data. The dashed curves denote the result of a calculation where $C^2S({}^8\text{He}/{}^6\text{He}_{0+}) = C^2S({}^8\text{He}/{}^6\text{He}_{2+}) = 1.0$.

local kernels was inadvertently left too large) which does not otherwise significantly affect the results presented there. The spectroscopic amplitudes for the $d + n$ overlap were fixed by setting the dominant S-wave component to 90% of the pure $d \otimes n$ value following [27] and adjusting the small D-wave component to give the D_2 value of [28]. The $n + {}^6\text{He}_{0+}$ spectroscopic amplitude was fixed by the spectroscopic factor obtained from the ratio of the measured decay width of the ${}^7\text{He}$ ground state to the pure single particle width calculated in a potential well using standard parameters [29]. As there is no empirical means of fixing the spectroscopic amplitudes for the $n + {}^6\text{He}_{2+}$ overlap we assumed a $1p_{3/2}$ configuration with a spectroscopic amplitude taken from the variational Monte Carlo (VMC) shell model calculation of [30]. This calculation also gives a $n + {}^6\text{He}_{0+}$ spectroscopic factor identical to that obtained from the measured decay width. The ${}^2n + p$ spectroscopic amplitude was fixed at unity and the ${}^2n + {}^6\text{He}_{0+}$ and ${}^2n + {}^6\text{He}_{2+}$ spectroscopic amplitudes adjusted to obtain the best fit to the data.

The calculations are compared with the transfer data in Figs. 2 and 3 and the best fit spectroscopic amplitudes are given in Table 2. The agreement between the calculations and both data sets is good. We emphasise that the only differences between the calculations at the two incident energies are the scattering potentials and the size of the deuteron breakup space. The improved agreement between calculation and data at angles greater than 50° for the ${}^8\text{He}(p, d){}^7\text{He}$ reaction at 15.7 A MeV compared to Skaza et al. [16] is mainly due to tuning the Koning and Delaroche potential used to construct the $d + {}^7\text{He}$ poten-

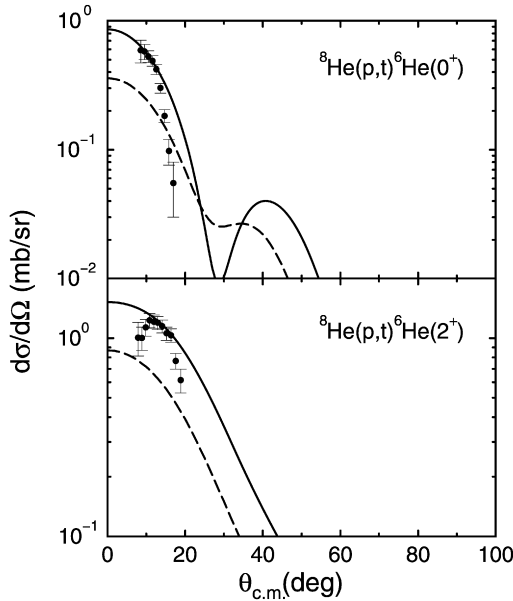


Fig. 3. CRC calculation at 61.3 A MeV compared to the ${}^8\text{He}(p,t){}^6\text{He}$ data of Korshennikov et al. [15]. The dashed curves denote the result of a calculation where $C^2S({}^8\text{He}/{}^6\text{He}_{0+}) = C^2S({}^8\text{He}/{}^6\text{He}_{2+}) = 1.0$.

Table 2
Spectroscopic amplitudes (SA) obtained from the CRC analysis

| Nucleus | Configuration | nlj | SA |
|-----------------|------------------------------|------------|---------------|
| ${}^8\text{He}$ | ${}^2n + {}^6\text{He}_{0+}$ | $2S_0$ | 1.0^a |
| ${}^8\text{He}$ | ${}^2n + {}^6\text{He}_{2+}$ | $1D_2$ | 0.12^a |
| ${}^8\text{He}$ | $n + {}^6\text{He}_{3/2-}$ | $1p_{3/2}$ | 1.7^a |
| ${}^7\text{He}$ | $n + {}^6\text{He}_{0+}$ | $1p_{3/2}$ | -0.728 [29] |
| ${}^7\text{He}$ | $n + {}^6\text{He}_{2+}$ | $1p_{3/2}$ | -1.327 [30] |

^a This work.

tials, the two-step transfer process having little effect on this reaction channel. We emphasise that this tuning of the potential does not significantly affect the cross section at angles smaller than 50° , most important for determining the spectroscopic factor.

It is apparent from Table 2 that, unlike the prediction of the COSMA model [15], we find a ${}^6\text{He } 2_1^+$ component of the ${}^8\text{He}$ ground state that is much smaller than the ${}^6\text{He } 0_1^+$ contribution. Nevertheless, our *absolute* spectroscopic amplitudes are consistent over two widely separated incident energies and we are able to describe the whole of the data—elastic scattering, one and two neutron pickup—at 15.7 A MeV. For comparison, we give the results of calculations where the spectroscopic amplitudes for the ${}^8\text{He}/{}^6\text{He}_{0+}$ and ${}^8\text{He}/{}^6\text{He}_{2+}$ overlaps have both been set to unity as the dashed curves in Figs. 2 and 3. While the descriptions of transfer leading to the ${}^6\text{He } 2_1^+$ state at 15.7 A MeV are comparable, it is clear that the dashed curves do not at all describe the transfer leading to the ${}^6\text{He } 0_1^+$ at either energy nor that to the ${}^6\text{He } 2_1^+$ state at 61.3 A MeV. However, these results may depend on the choice of $t + {}^6\text{He}$ optical potentials, which are not known. We therefore carried out a series of tests to investigate the sensitivity of our results to these quantities.

As the $t + {}^6\text{He}$ elastic scattering has not so far been measured we were forced to use the nearest available optical potentials as a basis for our calculations. While the potentials given in Table 1 do give very good consistency over the two incident energies, alternative potentials are available in the literature for the same data [24,25,31]. Potentials that give equivalent $t + {}^6\text{He}$ elastic scattering give similar results, regardless of potential “family” or whether the imaginary part is of surface or volume Woods–Saxon form. The effect of the choice of $t + {}^6\text{He}$ potential on the consistency of the spectroscopic amplitudes over the two incident energies is less conclusive. The ${}^8\text{He}/{}^6\text{He}_{2+}$ spectroscopic amplitudes are reasonably consistent at both energies provided that the $t + {}^6\text{He}$ potential for the calculation at 61.3 A MeV is consistent with the elastic scattering predicted by the potential of Bragin et al. [24]. The same is true for the ${}^8\text{He}/{}^6\text{He}_{0+}$ spectroscopic amplitudes if one takes the forward angle region at 15.7 A MeV where we unfortunately do not have data. Calculations at 61.3 A MeV that use potentials consistent with the $t + {}^6\text{He}$ elastic scattering given by the potentials of Burtebaev et al. [31] give spectroscopic amplitudes significantly larger than those obtained at 15.7 A MeV for both ${}^6\text{He}$ states. However, none of the potentials give results consistent with the COSMA prediction.

Test DWBA calculations did find a reasonably consistent value for the ratio of ${}^8\text{He}/{}^6\text{He}_{0+}$ to ${}^8\text{He}/{}^6\text{He}_{2+}$ spectroscopic factors over the two data sets, although the value varied from 1.1 to 2.2 depending on the exit channel potentials used. However, the absolute values for the ${}^8\text{He}/{}^6\text{He}_{0+}$ and ${}^8\text{He}/{}^6\text{He}_{2+}$ spectroscopic factors extracted from the DWBA analyses showed a very large range and were not at all consistent between the two incident energies, suggesting that the DWBA, with its assumption of weak coupling and a single-step reaction mechanism, is inadequate here.

To summarise, the consistency of our results over two widely spaced incident energies depends on the unknown $t + {}^6\text{He}$ potential. While it is true that none of our CRC calculations are consistent with the COSMA prediction for the ${}^8\text{He}/{}^6\text{He}_{0+}$ to ${}^8\text{He}/{}^6\text{He}_{2+}$ spectroscopic factor ratio a question mark must remain over our results until realistic $t + {}^6\text{He}$ potentials are available—this remark applies equally to DWBA analyses. This ambiguity could be removed by measurements of the appropriate elastic scattering in inverse kinematics; such measurements are in principle possible with a cryogenic tritium target. Obtaining data for transfer to the ${}^6\text{He } 0_1^+$ state over a larger angular range—forward angles at 15.7 A MeV to cover the first peak and at larger angles to define the second peak at 61.3 A MeV—would also remove some of the uncertainty in the present analysis. One might also question the use of a calculated spectroscopic amplitude for the $n + {}^6\text{He}_{2+}$ overlap; this procedure will only be as reliable as the calculation. However, the standard shell model using the Cohen and Kurath wave functions [30], the VMC shell model [30] and the TISM [13] all give reasonably similar results for this value, as they do for the $n + {}^6\text{He}_{0+}$ overlap, these latter in good agreement with the value extracted from the measured total decay width. Test calculations found that taking a smaller value for the $n + {}^6\text{He}_{2+}$ spectroscopic amplitude will yield a larger ${}^2n + {}^6\text{He}_{2+}$ spectroscopic amplitude;

taking a value for the $n + {}^6\text{He}_{2+}$ spectroscopic factor half that of the $n + {}^6\text{He}_{0+}$ one gives a ratio of ${}^8\text{He}/{}^6\text{He}_{0+}$ to ${}^8\text{He}/{}^6\text{He}_{2+}$ spectroscopic factors of 7, still much larger than the COSMA prediction of about 1.

In conclusion, we have obtained a consistent description of two data sets for the ${}^8\text{He}(p, t){}^6\text{He}$ reaction at widely differing incident energies with ${}^8\text{He} = {}^6\text{He}_{0+} + 2n$ and ${}^8\text{He} = {}^6\text{He}_{2+} + 2n$ spectroscopic factors of 1.0 and 0.014, respectively. The value for the ${}^8\text{He}/{}^6\text{He}_{0+}$ overlap is in remarkably good agreement with that obtained from a recent quasi-free scattering experiment [12], 1.3 ± 0.1 . Our value for the ${}^8\text{He}/{}^7\text{He}_{3/2-}$ spectroscopic factor, 2.9, is also in good agreement with the quasi-free scattering result, 3.3 ± 0.3 [12]. Our original CCBA analysis [17] of the ${}^8\text{He}(p, d){}^7\text{He}$ data concluded that the ${}^8\text{He}/{}^7\text{He}_{3/2-}$ spectroscopic factor obtained, 4.4 ± 1.3 , was consistent with a relatively pure $(1p_{3/2})^4$ configuration for the ${}^8\text{He}$ ground state, as assumed in the COSMA model. The final error bar, including all sources of uncertainty, was such that we were unable to draw a more definite conclusion. However, the current figure of 2.9—the reduction compared to the CCBA result is due to strong coupling effects taken into account by the CRC calculation—is significantly smaller than the sum-rule value and, combined with our results for the ${}^8\text{He}(p, t){}^6\text{He}$ reaction, enables us to be more specific. Our results suggest that the ${}^8\text{He}(p, t){}^6\text{He}$ reaction is a rather more sensitive probe of the ${}^8\text{He}$ ground state than the ${}^8\text{He}(p, d){}^7\text{He}$ neutron pickup, and that while the $(1p_{3/2})^4$ configuration is probably the dominant component of the ${}^8\text{He}$ ground state, there is a significant probability of finding the “valence” neutrons in other configurations such as $(1p_{3/2})^2(1p_{1/2})^2$, suggested in [12].

This result should, perhaps, not be surprising; assuming the ${}^8\text{He}$ ground state to consist of an α particle core plus four neutrons filling the $1p_{3/2}$ sub-shell is equivalent to assuming pure jj coupling. The intermediate coupling model of Cohen and Kurath [32] for the stable $1p$ -shell found that for the lighter nuclei, up to about $A = 9$, the coupling was actually very close to pure LS coupling, gradually changing to jj coupling as the mass increased through the shell. Our results provide new constraints for modern structure calculations, e.g. the *ab initio* shell model, which aim to describe the structure of light exotic nuclei. It will be interesting to see whether such calculations confirm the picture of a significant $(1p_{3/2})^2(1p_{1/2})^2$ component, for example, in the ${}^8\text{He}$ ground state.

Acknowledgements

N.K. gratefully acknowledges the receipt of a Marie Curie Intra-European Fellowship from the European Commission, contract No. MEIF-CT-2005-010158. K.W.K. acknowledges the support of the US National Science Foundation.

References

- [1] I. Tanihata, et al., Phys. Rev. Lett. 55 (1985) 2676.
- [2] I. Tanihata, et al., Phys. Lett. B 289 (1992) 261.
- [3] Y. Iwata, et al., Phys. Rev. C 62 (2000) 064311.
- [4] K. Varga, Y. Suzuki, Y. Ohbayasi, Phys. Rev. C 50 (1994) 189.
- [5] K. Varga, Y. Suzuki, R.G. Lovas, Nucl. Phys. A 571 (1994) 447.
- [6] Y. Suzuki, W.J. Ju, Phys. Rev. C 41 (1990) 736.
- [7] M.V. Zhukov, A.A. Korshennikov, M.H. Smedberg, Phys. Rev. C 50 (1994) R1.
- [8] A.V. Nesterov, V.S. Vasilevsky, O.F. Chernov, Phys. At. Nucl. 64 (2001) 1409.
- [9] T. Kobayashi, et al., Phys. Rev. Lett. 60 (1988) 2599.
- [10] R.E. Warner, Phys. Rev. C 55 (1997) 298.
- [11] K. Markenroth, et al., Nucl. Phys. A 679 (2001) 462.
- [12] L.V. Chulkov, et al., Nucl. Phys. A 759 (2005) 43.
- [13] R. Wolski, et al., in: A. Ohnishi, N. Itagaki, Y. Kanada-En'yo, K. Kato (Eds.), Clustering Aspects of Quantum Many Body Systems, Kyoto, 12–14 November 2001, World Scientific, 2002, p. 15.
- [14] D.D. Bogdanov, et al., in: Yu.E. Penionzhkevich, E.A. Cherepanov (Eds.), International Symposium on Exotic Nuclei, Lake Baikal, 24–28 July 2001, World Scientific, 2002, p. 229.
- [15] A.A. Korshennikov, et al., Phys. Rev. Lett. 90 (2003) 082501.
- [16] F. Skaza, et al., Phys. Lett. B 619 (2005) 82.
- [17] F. Skaza, et al., Phys. Rev. C 73 (2006) 044301.
- [18] H.R. Weller, et al., Phys. Rev. C 18 (1978) 1120.
- [19] I.J. Thompson, Comput. Phys. Rep. 7 (1988) 167.
- [20] J.-P. Jeukenne, A. Lejeune, C. Mahaux, Phys. Rev. C 16 (1977) 80.
- [21] A.J. Koning, J.P. Delaroche, Nucl. Phys. A 713 (2003) 231.
- [22] A.M. Eiró, I.J. Thompson, Phys. Rev. C 59 (1999) 2670.
- [23] P. Guazzoni, et al., Phys. Rev. C 69 (2004) 024619.
- [24] V.N. Bragin, et al., Sov. J. Nucl. Phys. 44 (1986) 198.
- [25] A.K. Basak, et al., Nucl. Phys. A 368 (1981) 74.
- [26] D.T. Khoa, W. von Oertzen, Phys. Lett. B 595 (2004) 193.
- [27] M.F. Werby, S. Edwards, Phys. Rev. C 8 (1973) 978.
- [28] C.M. Bhat, et al., Phys. Rev. C 38 (1988) 1537.
- [29] G. Rogachev, private communication.
- [30] A.H. Wuosmaa, et al., Phys. Rev. C 72 (2005) 061301(R).
- [31] N. Burtebaev, et al., Phys. At. Nucl. 58 (4) (1995) 596.
- [32] S. Cohen, D. Kurath, Nucl. Phys. A 101 (1967) 1.